

Redox Activating Dip Pen Nanolithography (RA-DPN)
Adam B. Braunschweig, Andrew J. Senesi, Chad A. Mirkin*

Materials and Methods.

Aminopropyl trimethoxysilane (APTMS), 1,4-benzoquinone, ceric ammonium nitrate (CAN), analytical grade ethanol, and sodium ascorbate were purchased from Aldrich and used as received. Nucleotides were purchased from Glen Research and used as received. Silicon wafers (Si 100) with a 525 nm thermal oxide layer were purchased from Siltronic AG. Solutions were prepared from Nanopure water purified with Milli-Q plus system (Millipore Co.), with a resistivity over 18 MΩcm. Anti-cholera toxin β was purchased from Invitrogen, Inc. and used as received. DPN experiments were carried out using an NSCRIPTOR II DPN system (NanoInk, Inc.) with F type 26 pen tip arrays (NanoInk, Inc.). Atomic force microscopy imaging was carried out on a Dimension 3100 atomic force microscope (Veeco Metrology Group) with Pointprobe plus Si SPM sensors (Nanosensors, Inc.). Epifluorescence microscopy images were taken with a Zeiss Axiovert 200M microscope. IR spectra were taken on a Nexus 870 FTIR spectrometer (Thermo Nicolet) equipped with a MCT detector and a GATR attenuated total reflectance cell from Harrick Scientific. Raman spectra were taken on a Witec Raman microscope with 633 nm excitation. The oligonucleotides were synthesized on a Nucleic Acid Synthesis System (Expedite) and purified on a Prostar HPLC system (Varian), and had a sequence of 3' Cy3 CTC CAC AGG AGT CAG GTG CAC TTT TTT TTT T NH₂ 5'.

Surfaces were prepared by first immersing a Si/SiO₂ wafer in a piranha solution at 60 °C for 45 min. The wafers were washed with water and ethanol, and then dried under a stream of nitrogen. In an oxygen and water free environment, the Si/SiO₂ surfaces were immersed in a 2% (v/v) solution of APTMS in dry toluene for 5 h. The surfaces were washed with toluene and ethanol, and immersed in a 5 mM solution of freshly sublimed 1,4-benzoquinone at 60 °C for 8 h. The surfaces were subsequently washed with ethanol and dried under a nitrogen stream.

To ink the cantilever arrays for RA-DPN with CAN, parafilm was used to sandwich the chip holding the array of 26 cantilevers (F26 pen array, NanoInk, Inc) so that the CAN solution deposited by micropipette would be localized on the cantilevers.^{S1} Drying the array in a water vapor saturated oven resulted in an even coating of the CAN oxidant on the tips, as evidenced by optical microscopy (Figure S1), when compared to an unlinked cantilever array (Figure S2).

Prior to patterning, the surfaces were first reduced by immersing quinone-coated silicon surfaces in a 5 mM aqueous solution of sodium ascorbate for 15 min, washing with water, and drying with a nitrogen stream (see below for further discussion of switching). The surfaces were placed in an environmental chamber at a relative humidity of 40-60 %. Delivery of the CAN to the surface was carried out in contact mode at ambient temperature. Dot patterns were created using InkCAD software that allows for control over dwell times and position. Surfaces were subsequently washed with water and immersed in a 10 μM oligonucleotide or 50 μg mL⁻¹ protein solution for 1.5 hours. The surfaces were washed with water and sonicated 30 min prior to fluorescence imaging.

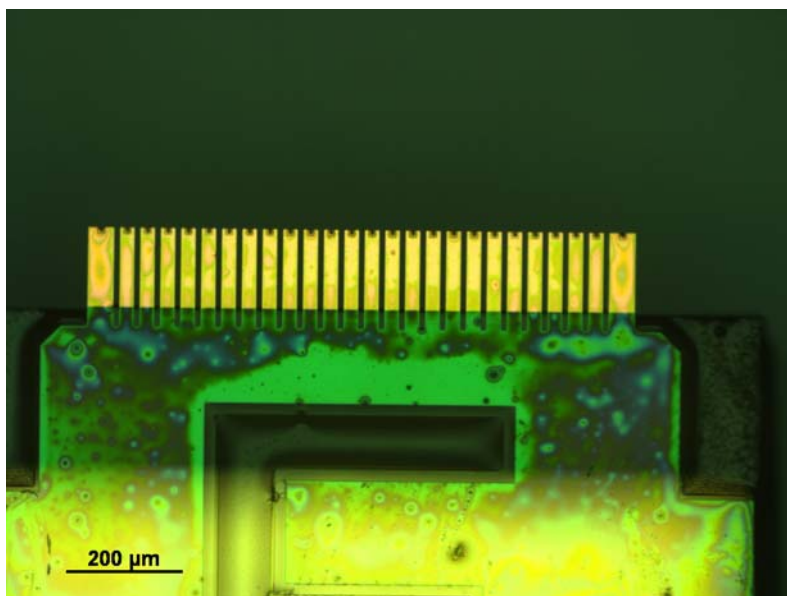


Figure S1. Optical microscopy image of F-type tip arrays that show an even coating of the ink CAN following the inking protocol.

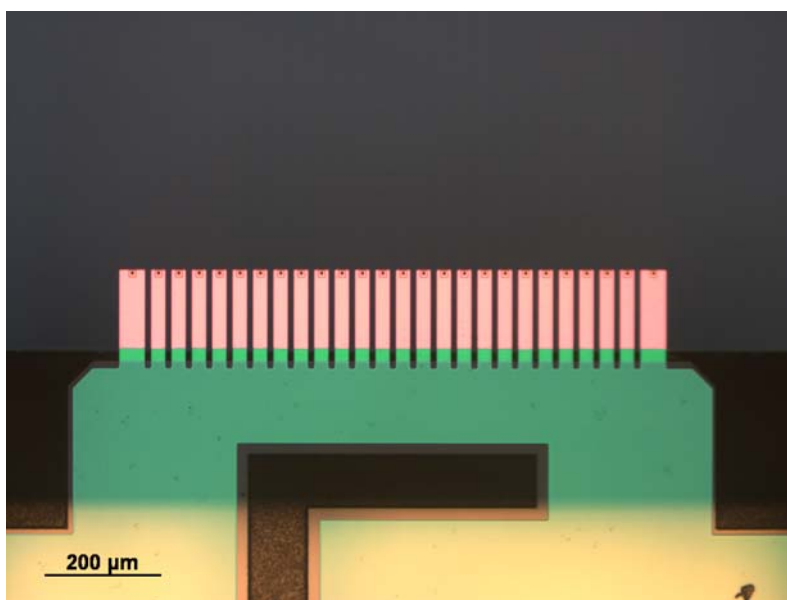


Figure S2. Optical microscopy image of clean F type tip arrays prior to inking protocol.

Spectroscopic Surface Characterization.

The formation of the quinone-terminated surface was characterized by X-ray photoelectron spectroscopy (XPS), Raman spectroscopy, and infrared (IR) spectroscopy. Elemental analysis of the functionalized surface was carried out with XPS. Following reaction of the Si/SiO₂ surface with APTMS and the quinone, a prominent N^{1s} peak appeared at 406.6 eV (Figure S3). Also, the intensity of the C^{1s} peak at 292.2 eV increases significantly. These results indicate the formation of an organic coating on the SiO₂ surface after the reaction with APTMS. The quinone surface showed characteristic^{S2} FTIR peaks (Figure S4) at 2849 cm⁻¹ (CH symmetric stretch), 2918 cm⁻¹ (CH asymmetric stretch in the prominent aliphatic region) and 2970 cm⁻¹ (conjugated alkene CH stretch), confirming the presence of both the propyl and aromatic groups on the surface. Raman peaks (Figure S5) confirmed the presence of the aliphatic CH stretches (1407, 1424, 1480 cm⁻¹) as well as the quinone moiety (1535 cm⁻¹, 1576 cm⁻¹ and 1620 cm⁻¹). Notably, the Raman spectra indicate the presence of both monoamino- (1620 cm⁻¹) and diamino- (1576 cm⁻¹) substituted benzoquinone on the surface according to previously reported assignments.^{S2}

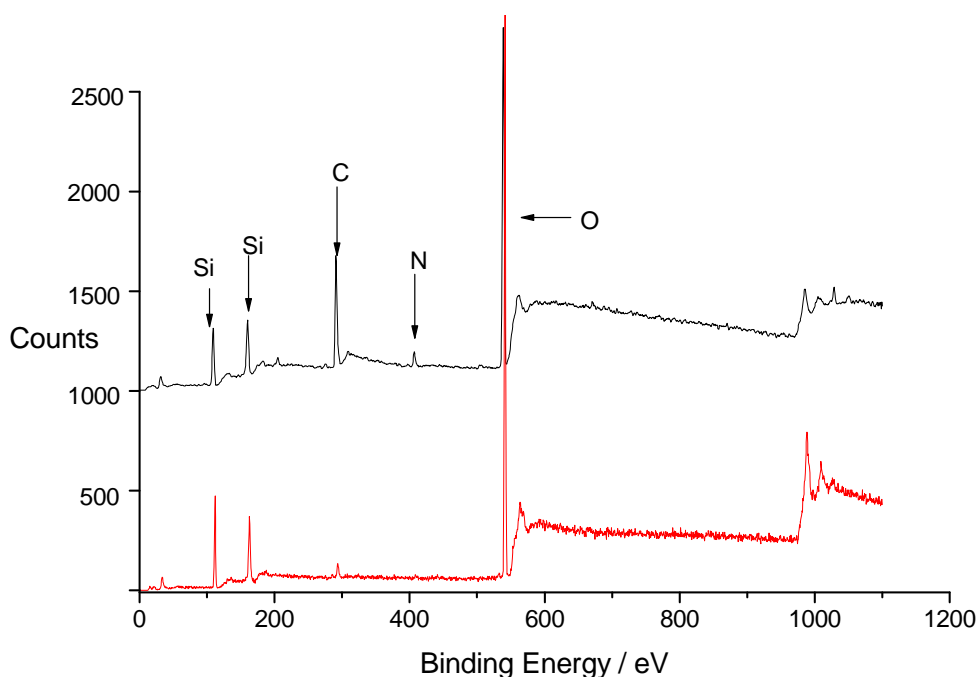


Figure S3. X-ray Photoelectron Spectroscopy (XPS). The XPS spectra of the bare Si/SiO₂ wafer (red) and the quinone functionalized Si/SiO₂ wafer (black) are shown. The emergence of the Nitrogen peak and the increase in intensity of the Carbon peak indicate that the silane modification with aminopropyl trimethoxysilane occurred successfully. Black spectrum has been offset by 1000 counts.

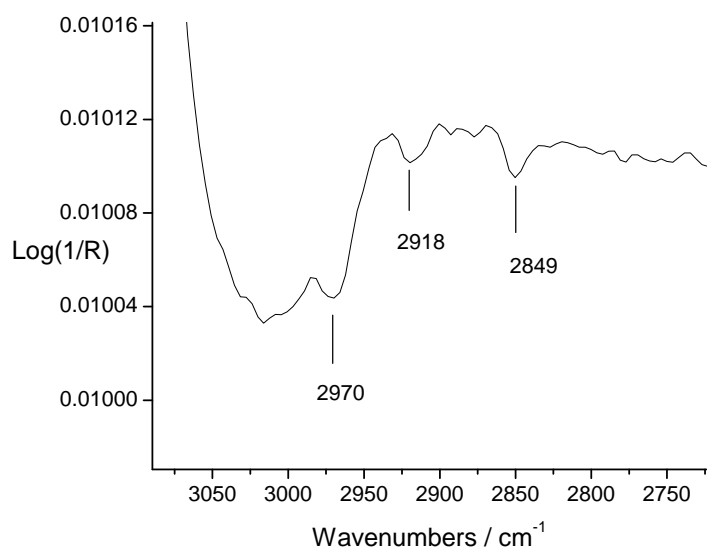


Figure S4. ATR-FTIR spectrum of quinone monolayers on Si/SiO₂ spectra. A bare Si/SiO₂ wafer was used as a background. The peaks at 2849 cm⁻¹ (CH asymmetric stretch) and 2918 cm⁻¹ (CH asymmetric stretch) indicate the presence of aliphatic chains on the surface, and the peak at 2970 cm⁻¹ (alkene CH stretch) indicates the presence of a quinone moiety on the surface.

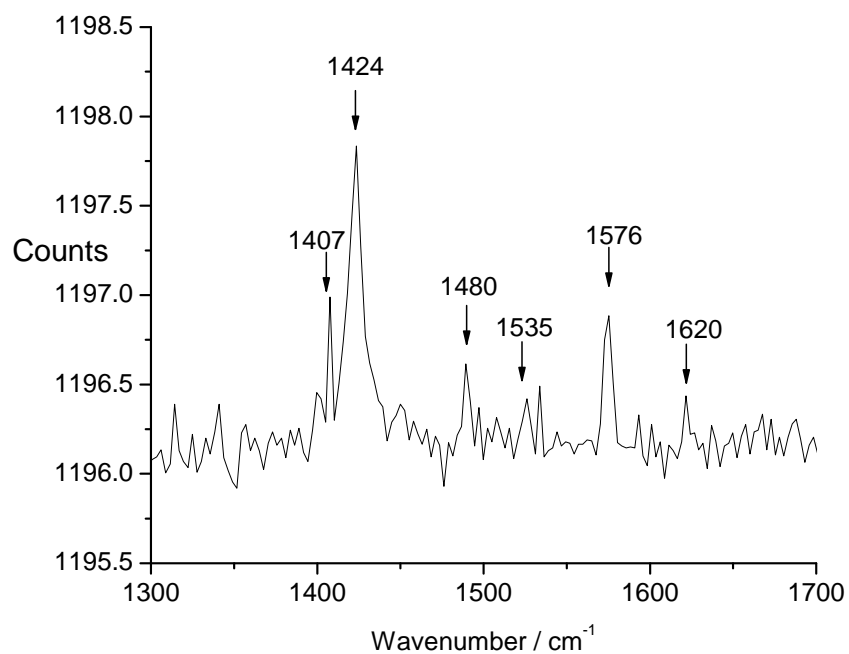


Figure S5. Raman spectrum of the benzoquinone modified Si/SiO₂ surface. Excitation was induced with a 633 nm laser. Peaks at 1407, 1424 and 1480 cm⁻¹ correspond to aliphatic C-H stretches. Peaks at 1535, 1576 and 1620 cm⁻¹ have been assigned previously to quinone moieties. Additionally, the peak at 1576 cm⁻¹ has been assigned to monoamino benzoquinone, and the peak at 1620 cm⁻¹ has been assigned to the diamino quinone. Assignments are based on the Raman characterization of a quinone functionalized cysteine monolayer in reference S2.

Surface Switching.

The conversion between hydroquinone and benzoquinone forms was reversibly induced with chemical reagents and monitored by contact angle measurements (Figure S5). It has been shown previously,^{S3} that the oxidized benzoquinone form has a larger contact angle than the reduced hydroquinone form. The switching was induced by immersing the hydrophilic hydroquinone surface ($30^\circ \pm 2$) in a 5 mM aqueous solution of CAN. Following subsequent immersion of the oxidized surface in a 5 mM aqueous solution of the reducing agent sodium ascorbate, the contact angle returned to its original value of $24^\circ \pm 1$. This reversible switching could be reproduced over several cycles. The contact angle data confirm that the surface functionality can be switched between hydroquinone and benzoquinone forms by the site-specific delivery of redox agents and is the pattern forming mechanism.

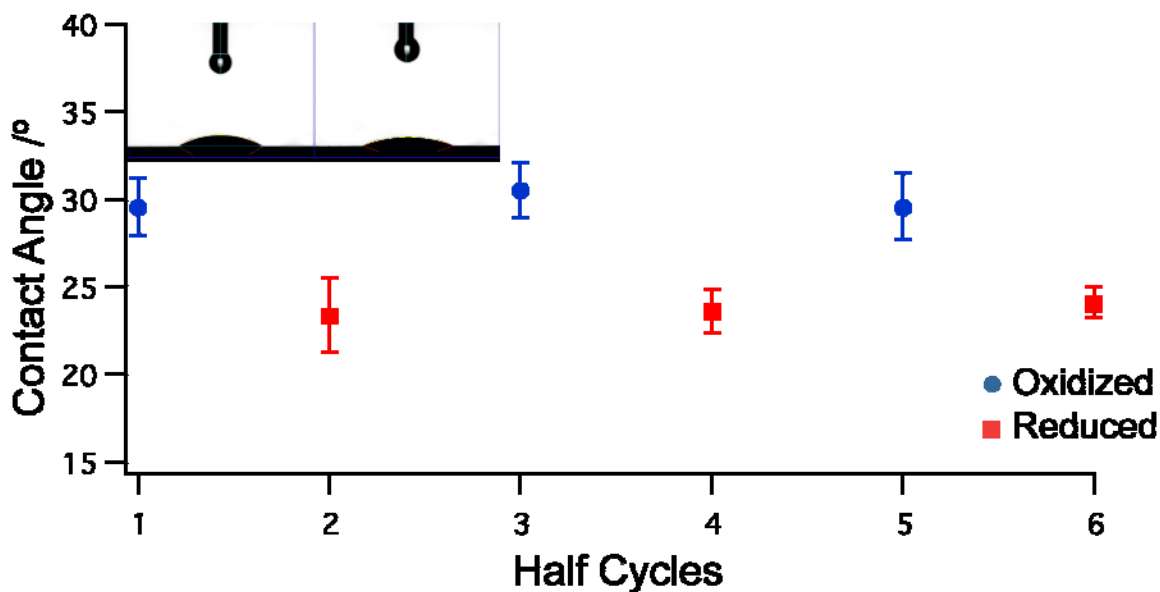


Figure S6. Surface Characterization. Contact angle showing reproducible chemical switching capability of the quinone surface. Left insert, image of benzoquinone (BQ) surface; right insert, image of hydroquinone (HQ) surface. Reduction of the surface to the hydroquinone form was induced by immersing the surface in a 5 mM aqueous solution of sodium ascorbate. The surface was oxidized by immersion in a 5 mM aqueous solution of CAN.

AFM Images.

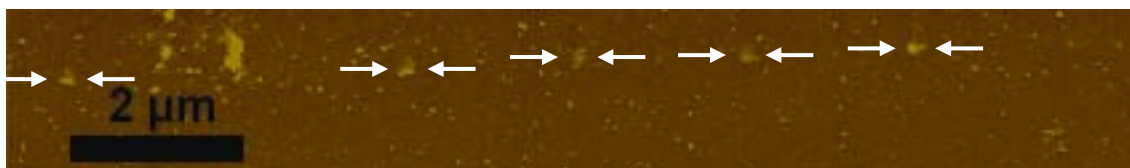


Figure S7. AFM height image of 165 nm oligonucleotide features created by RA-DPN.

Epifluorescence Images.

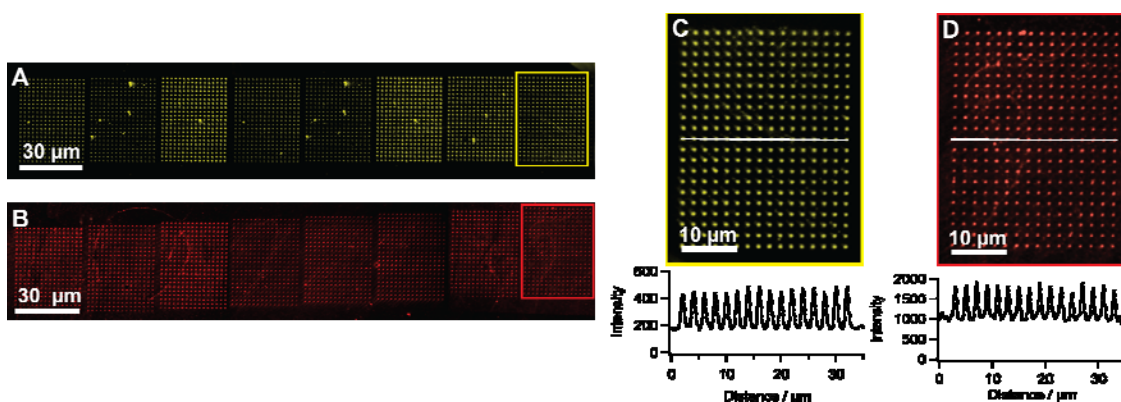


Figure S8. Epifluorescence images of DNA and proteins made using the RA-DPN method. (A) 16 x 21 dot patterns of Cy3 labeled aminated DNA made with a 26 pen F type cantilever array (NanoInk, Inc.). (B) 16 x 21 dot patterns of AF549 labeled cholera toxin β subunit made with a 26 pen F type cantilever array. (C) Zoomed in view of one 16 x 21 dot array of the oligonucleotide dots. Below is shown a plot of the intensity profiles of the dots with an average signal to noise ratio of 2.4 : 1. (D) Zoomed in view of one 16 x 21 dot array of the protein dots. Below is shown a plot of the intensity profiles of the dots with an average signal to noise ratio of 2 : 1.

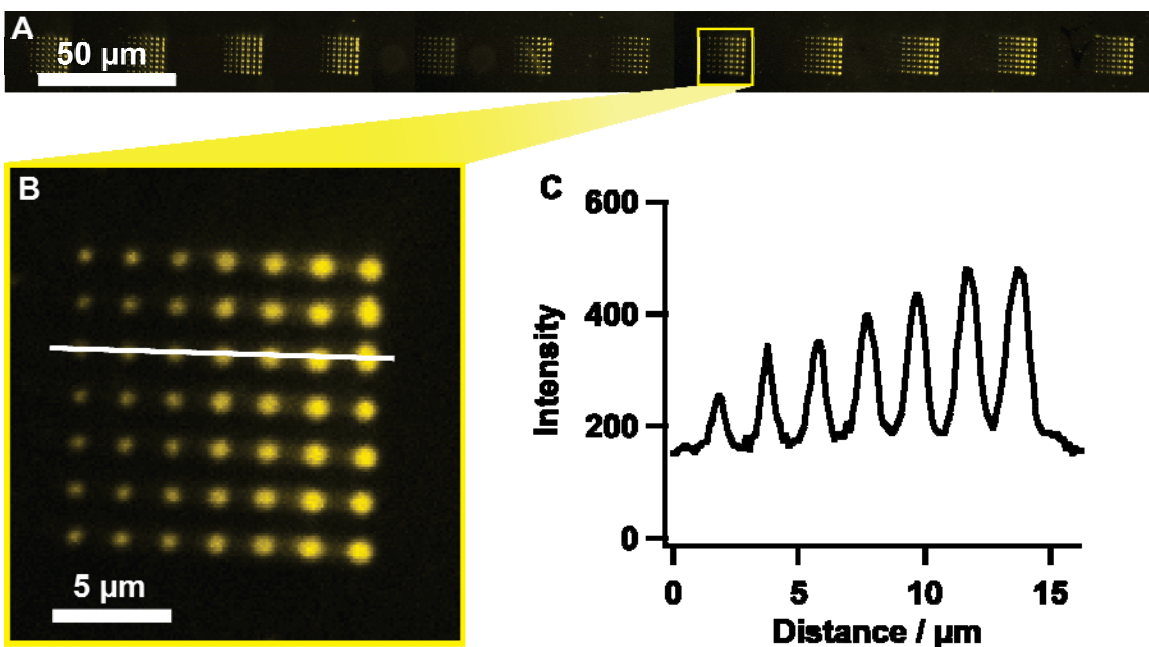


Figure S9. Epifluorescence image of Cy3 labeled protein dots (A) made with 26 pen F arrays. Dwell times were increased from left to right. (B) Magnified view of a single array. (C) Profile of fluorescence intensity for the DNA pattern magnified in image (B).

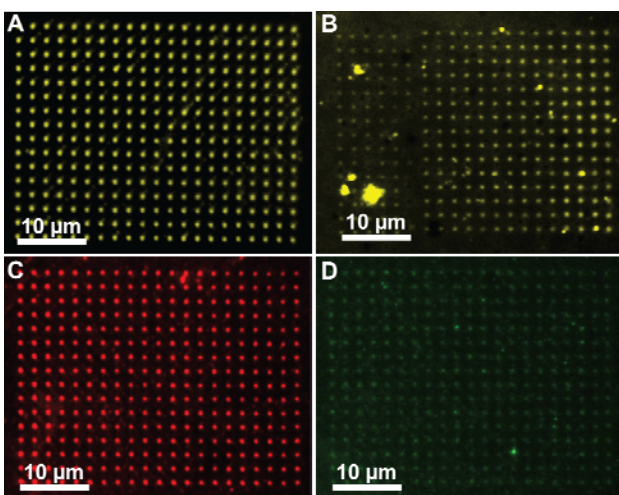


Figure S10. Epifluorescence images of (A) Cy3-labeled DNA on an Si/SiO₂ surface, (B) Cy3 labeled DNA on a glass surface, (C) AF549 labeled cholera toxin β subunit on a Si/SiO₂ surface, and (D) binding of the AF488 labeled antibody to cholera toxin β subunit printed surface.

References.

(S1) Wang, W. M.; Stoltenberg, R. M.; Liu, S.; Bao, Z. *ACS Nano* **2008**, 2, 2135– 2142.

(S2) (a) Sarkar, S.; Sampath, S. *Langmuir* **2006**, 22, 3388 – 3395. (b) Sarkar, S.; Sampath, S. *Langmuir* **2006**, 22, 3396 – 3403.

(S3) Wieckowska, A.; Braunschweig, A. B.; Willner, I. *Chem. Commun.* **2007**, 3918 – 3920.